

## Microscopic origins of first-order Sm-A–Sm-C phase behavior in de Vries smectic liquid crystals

Zachary V. Kost-Smith,<sup>1,2</sup> Paul D. Beale,<sup>1</sup> Noel A. Clark,<sup>1,2</sup> and Matthew A. Glaser<sup>1,2,\*</sup>

<sup>1</sup>*Department of Physics, University of Colorado, Boulder, Colorado 80309, USA*

<sup>2</sup>*LCMRC, University of Colorado at Boulder, Boulder, Colorado 80309, USA*

(Received 14 December 2012; published 28 May 2013)

We explore the phase behavior of tilted hard rods as a model of de Vries smectic behavior and the first order smectic-C (Sm-C) to smectic-A (Sm-A) phase transition. The free energy cost of azimuthal rotation of a molecule away from the local tilt direction is calculated via umbrella sampling. This calculation is used to map the hard rod system onto a lattice spin system which shows a cross-over from a continuous to first-order phase transition as the tilt of the rods is increased. This analysis offers a natural explanation of the first-order Sm-A–Sm-C phase transition common to de Vries smectics.

DOI: [10.1103/PhysRevE.87.050502](https://doi.org/10.1103/PhysRevE.87.050502)

PACS number(s): 64.70.M–, 61.30.Cz, 61.30.Gd

In 1977, de Vries reported a new type of liquid-crystal Sm-A phase that showed a set of qualitatively different features from the conventional Sm-A phase [1–3]. Initially this phase was distinguished from other smectics by a first-order Sm-A–Sm-C phase transition with an anomalously small reduction in layer spacing [4]. Subsequent work showed the characteristics of the de Vries Sm-A phase also includes large electroclinic responses [5], large field-driven changes in birefringence in chiral materials [6], and a lack of a nematic phase in the phase sequence. One of de Vries' early models, now called the hollow cone model, proposed that these phases are smectics with a molecular orientational distribution which is uniform in azimuthal angle  $\phi$  but has a preferred tilt away from the layer normal,  $\theta_A$ , sweeping out the surface of a cone, Fig. 1. While this model remains controversial, it neatly explains the electro-optic response of chiral de Vries systems as well as the small layer contraction as the effects of averaging the molecular properties over azimuthal angle [7].

Although many of the features of the de Vries Sm-A phase can be explained by applying the hollow cone model, the observations of a first-order Sm-A–Sm-C transition [1,5] remain unexplained despite substantial study of these systems. In this paper we show using simulations and mean-field theory that much like the anomalous layer spacing and electro-optic response, the first-order Sm-A–Sm-C phase transition seen in de Vries smectics can be understood as a direct result of the hollow cone model.

Materials exhibiting de Vries phases sparked interest for use in ferroelectric liquid-crystal displays [8]. The small change in layer spacing makes these good candidates for ferroelectric liquid-crystal (FLC) displays where large changes to that spacing can cause the formation of “zig-zag” defects during manufacturing [9]. In addition, the large electroclinic effect of de Vries Sm-A phases is well suited for sensitive chirality detection [5]. These potential applications have led to substantial research attempting to characterize and understand de Vries behavior which in turn has led to empirical exploration of the properties of de Vries materials. For instance, liquid crystal chemists discovered that chemical and structural motifs that promote layering, such as polyphilic or bulky tails, tend to produce de Vries-like behavior. This has given us

some degree of predictive power in the design of de Vries mesogens [10]. The correlation between strong layering and de Vries materials also manifests as a direct isotropic to Sm-A phase transition, bypassing the nematic phase entirely. Meanwhile, high-resolution x-ray studies of the Sm-A–Sm-C phase transition have directly observed a discontinuous change in layer spacing in several materials [5,11]. Exploration of the electro-optic behavior reveals a distinct sigmoidal polarization response, or double-peaked polarization current response [7,12–15] in a broad range of de Vries materials, also indicative of a first-order Sm-A–Sm-C phase transition. This first-order phase transition is in sharp contrast to the second-order Sm-A–Sm-C transition common in conventional smectics [1,16].

Several groups have performed theoretical studies of the de Vries Sm-A phase and the Sm-A–Sm-C transition at a phenomenological level. Bahr *et al.* used a simple Landau theory to model de Vries-like electroclinic response seen in material C7 [12]. The mean-field theory developed by Saunders *et al.* shows that coupling between tilt and biaxiality in smectics can produce a first-order Sm-A–Sm-C phase transition, but does not point to a microscopic origin for this coupling [17,18]. In a similar vein, work by Gorkunov *et al.* shows that the addition of higher order coupling terms into a mean-field theory recreates the anomalously small change in layer spacing through the Sm-A–Sm-C phase transition, and shows how these couplings might arise based on a model of intermolecular interaction [19,20]. At the microscopic level, Lagerwall *et al.* have proposed an alternative to the hollow cone model based on a conventional Sm-A with abnormally low nematic order [21].

Our work starts from the microscopic foundation of the hollow cone model and explores the implications of this model for de Vries smectics using Monte Carlo simulations, umbrella sampling, coarse-graining, and mean-field techniques. This bottom-up analysis culminates in the realization that the first-order Sm-A–Sm-C transition can be viewed as a consequence of the hollow cone model via a defect condensation mechanism.

We begin by considering the behavior of a hollow cone fluid of a single smectic layer of hard spherocylinders. We performed NPT Monte Carlo simulations of a fluid of spherocylinders which are confined to the  $z = 0$  plane and tilted from the layer normal by fixed cone angle  $\theta_A$ , but

\*matthew.glaser@colorado.edu

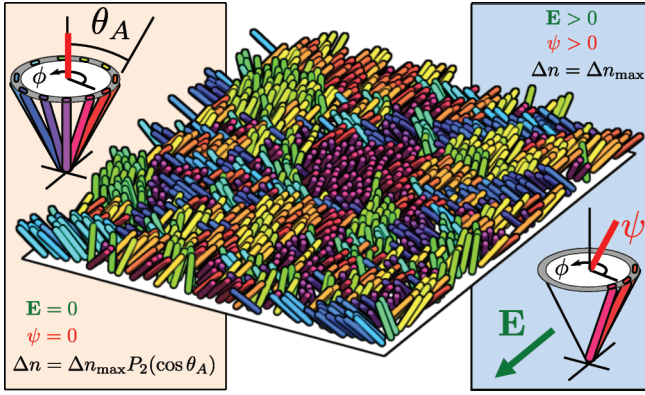


FIG. 1. (Color online) Snapshot from a Monte Carlo simulation of a single-layer hard spherocylinder smectic with the hollow cone orientation distribution (color represents azimuthal orientation). This NPT simulation was performed with cone angle  $\theta_A = 45^\circ$  and spherocylinder length  $L/D = 5$  in the Sm-A phase near the Sm-A–Sm-C phase transition. Molecules in the hollow cone model have the orientation distribution in tilt  $\theta$  and azimuthal angle  $\phi$  of the form  $f(\theta, \phi) = (2\pi)^{-1}g(\theta)$ . The distribution is uniform in  $\phi$  while  $g(\theta)$  is narrowly peaked around the cone angle  $\theta_A$ , which we take as the delta function  $\delta(\theta - \theta_A)$ . Hollow cone smectics show no global polar order in the Sm-A phase but produce finite correlated regions. Macroscopic tilt  $\psi$  is the result of global bias of molecules to one side of the  $\phi$  distribution.

allowed to freely rotate in azimuthal angle  $\phi$ . This rigid realization of the hollow cone model where the distribution of spherocylinders in  $z$  and  $\theta_A$  are explicitly  $\delta$  functions is chosen to reduce the number of free parameters in the model. A more realistic model would include out-of-layer fluctuations and a finite distribution in angle  $\theta$  centered around the cone angle, but such generalizations should not change the qualitative conclusions of the analysis.

The pressure in the simulation is equivalent to an effective mean attraction between the spherocylinders, mapping the hard core system onto a thermotropic system with temperature inversely proportional to pressure. At sufficiently large cone angles, simulations of this idealized system show a first-order phase transition between a quasi-long-ranged Sm-C–like phase at high pressure (low temperature) and a disordered phase at low pressure (high temperature) where finite  $\phi$ -correlated domains average to Sm-A symmetry as demonstrated in Fig. 1. These domains occur in hollow cone smectics due to the effective potential experienced by tilted spherocylinders interacting with their neighbors. The existence of these correlated domains predicts very different behavior from conventional Sm-A phases. Specifically, whereas fields on conventional Sm-A phases act on single molecules resulting in weak electroclinic coupling, the electroclinic effect due to reorienting the  $\phi$  value of correlated domains around the cone is much larger. This is particularly noticeable near the Sm-A–Sm-C phase transition, which is consistent with experimental measurements of de Vries systems [5].

We measure the effective azimuthal potential by computing the Gibbs free energy cost of rotating a single spherocylinder by angle  $\Delta\phi$  away from the local azimuthal order averaged over a domain of radius  $a$  in the fluid layer,  $G(\Delta\phi)$ . An umbrella sampling scheme ensures proper sampling over

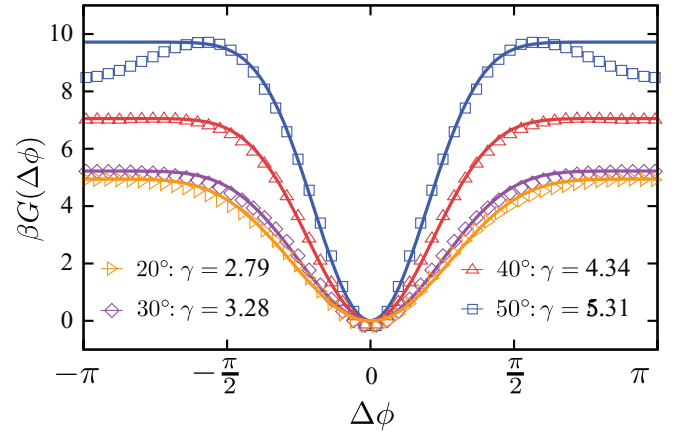


FIG. 2. (Color online) Umbrella sampling calculations of the Gibbs free energy of azimuthal rotation within a smectic layer of a single spherocylinder relative to the polarization vector averaged among surrounding spherocylinders within radius  $a = 5\sigma$  where  $\sigma$  is the spherocylinder diameter. These calculations are performed within the Sm-C phase near the Sm-A–Sm-C phase transition at different cone angles  $\theta_A$ . At larger cone angles a secondary minimum appears at  $\phi = \pi$ . Superimposed are fits of the  $\gamma$  potential, Eq. (1), where the secondary minimum is excluded from the fitting procedure if present by separately fitting  $G_{\max}$  as demonstrated in the  $50^\circ$  fit. As the cone angle is increased the width of the well is reduced, or equivalently,  $\gamma$  increases.

the full range of the rotational potential. We make iterative approximations to  $G(\Delta\phi)$  in order to bias the system away from well-sampled regions. Each iteration improves the approximation by using the sampled histogram  $\rho^{(i)}(\Delta\phi)$  via the equation

$$G^{(i)}(\Delta\phi) = -k_B T \ln[\rho^{(i-1)}(\Delta\phi)],$$

where the superscripts denote the iteration. The free energy profile, demonstrated in Fig. 2 for various cone angles in the Sm-C phase near the Sm-A–Sm-C transition, shows a narrow minimum at  $\Delta\phi = 0$  whose width decreases with increasing cone angle. This result is robust to changes in the hollow cone  $\theta$  distribution. For instance, defining a diffuse hollow cone via a harmonic potential in the  $\theta$  coordinate produces qualitatively similar results.

Using the free energy profile and our observation that this system is well represented as a collection of  $\phi$ -correlated domains, we define a coarse graining transformation which maps our off-lattice hollow cone smectic onto a generalized XY spin model with lattice constant  $a$ , the coarse-graining length scale. The average  $\phi$  coordinate of the correlated domains within the smectic layer maps to the spin orientations in the XY model and the free energy profile maps to the in-layer nearest-neighbor interaction. Motivated by this measured azimuthal free energy curve, we choose an in-layer potential of the form

$$U_{ij} = -J_{xy} \left[ \frac{1}{2} [\cos(\phi_i - \phi_j) + 1] \right]^\gamma. \quad (1)$$

This potential, which we call the  $\gamma$  potential, features an energy minimum at  $\Delta\phi = 0$  whose width is tuned via parameter  $\gamma$ . The  $\gamma$  potential fits well to the free energy profile at small to moderate cone angles near the Sm-A–Sm-C phase

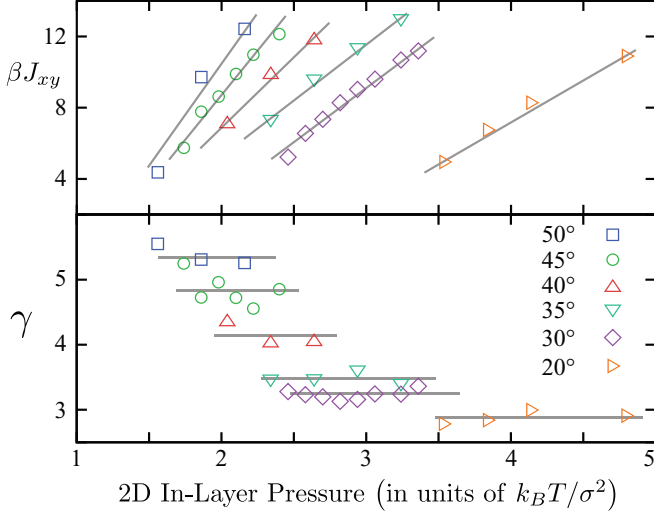


FIG. 3. (Color online) Mapping between the hard spherocylinder hollow cone system and the  $\gamma$ -potential XY model when using  $a = 5\sigma$  as the coarse-graining length scale where  $\sigma$  is the diameter of the spherocylinders. Spin coupling strength  $J_{xy}$  increases approximately linearly with pressure, while the  $\gamma$  values are nearly independent of pressure but increase with larger cone angles  $\theta_A$ . While the specific values of  $J_{xy}$  and  $\gamma$  depend on  $a$ , these trends do not.

transition as shown in Fig. 2. At larger cone angles we observe a secondary minimum at  $\Delta\phi = \pi$  which we choose to exclude from the fitting procedure because our analysis suggests that the width of the minimum at  $\Delta\phi = 0$  is the essential feature of the interaction. At sufficiently large cone angles, however, we predict that de Vries systems might additionally exhibit a smectic phase with two-dimensional nematic order of the  $c$ -director analogous to the phase reported in spin systems with a secondary minimum [22].

These fits provide us with a map, summarized in Fig. 3, between our hard spherocylinder system governed by pressure, spherocylinder length, and cone angle to a spin system of lattice constant  $a$  governed by the angular width of the minimum in the neighbor interaction potential (encoded in  $\gamma$ ) and the dimensionless energy ratio  $\beta J_{xy}$ . With respect to pressure, the map reveals a roughly linear increase of the coupling strength  $J_{xy}$  and approximately constant  $\gamma$  independent of cone angle. We note that while the energy ratio  $\beta J_{xy}$  corresponding to the transition shows no real trend with respect to cone angle, the value of  $\gamma$  shows a distinct increase as the angle increases.

The  $\gamma$  potential can be viewed as a continuous version of the Potts model interaction  $u(\phi_i, \phi_j) = -J\delta_{\phi_i, \phi_j}$ , where  $\delta_{\phi_i, \phi_j}$  is the Kronecker delta over possible discrete  $\phi$  states. Previous work by Domany *et al.* on two-dimensional spin systems used the  $\gamma$  potential to explore the cross-over between the continuous Kosterlitz-Thouless phase transition of the planar rotor XY model with interaction  $u(\phi_i, \phi_j) = -J\cos(\phi_i - \phi_j)$  at  $\gamma = 1$  and the first-order phase transition of the  $n$ -state standard Potts model where  $n > 4$  [23].

Our de Vries system is composed of smectic layers which, like the two-dimensional spin systems of Domany *et al.*, are represented as planes of spin coupled by the  $\gamma$  potential of strength  $J_{xy}$  in the  $x$  and  $y$  directions. The spins in these layers interact with adjacent layers in the  $z$  direction via a planar

rotor style coupling of strength  $J_z$ . The Hamiltonian for this anisotropic cubic XY model is given by Eq. (2) where we have assumed integer  $\gamma$ , expressed the  $\gamma$  potential as a finite Fourier sum with known coefficients  $b_k$ , and sum the last term over all in-layer neighbors.

$$H = -pE \sum_i \cos(\phi_i) - J_z \sum_i \cos(\phi_i - \phi_{i+1}) - J_{xy} \sum_{(i,j)} \sum_{k=1}^{\gamma} b_k \cos[k(\phi_i - \phi_j)]. \quad (2)$$

We characterize the phase behavior of our related system using self-consistent variational mean-field theory [24]. In the mean-field approximation we absorb the lattice's geometric factors into our coupling constants and combine the planar rotor interlayer coupling with the first term of the in-layer coupling. We assume that the  $N$ -spin matrix can be written as the product of single-spin density matrices, Eqs. (3) and (4). Sets of order parameters  $c_k$  are found that satisfy the  $\gamma$  different self-consistency constraints in Eq. (5). The stable phase is parametrized by the set of order parameters minimizing the mean free energy, Eq. (6).

$$\rho_1 = \frac{1}{Z_1} \exp \left[ \beta \left( pE + \sum_k J_k c_k \cos(k\phi) \right) \right], \quad (3)$$

$$Z_1 = \int_0^{2\pi} \exp \left[ \beta \left( pE + \sum_k J_k c_k \cos(k\phi) \right) \right] d\phi, \quad (4)$$

$$c_k = \int_0^{2\pi} \rho(\phi) \cos(k\phi) d\phi, \quad (5)$$

$$F = \frac{1}{2} N \sum_k J_k c_k^2 - \frac{N}{\beta} \ln(Z_1). \quad (6)$$

The system shows a transition between the paramagnetic (Sm-A) phase and ferromagnetic (Sm-C) phase as shown in the  $\gamma$ - $T$  phase diagram in Fig. 4. Much like Domany

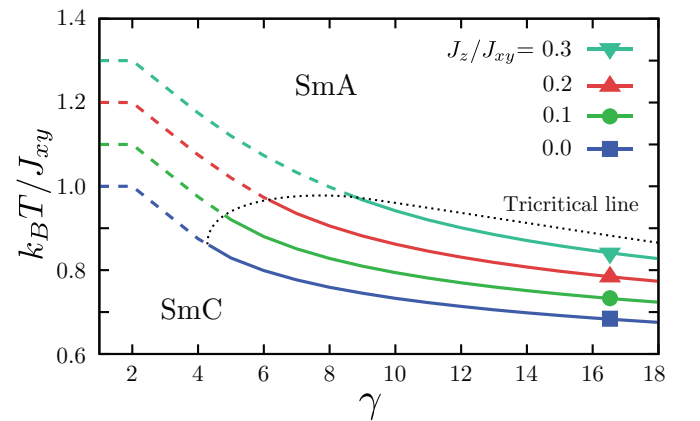


FIG. 4. (Color online)  $\gamma$ - $T$  phase diagram of the  $\gamma$ -potential spin system showing tricritical behavior. The dashed and solid phase boundaries denote second- and first-order phase transitions, respectively. In the two-dimensional system (■) and systems with weak interlayer coupling,  $J_z/J_{xy} < 0.1$ , the phase transition crosses over from continuous to first order between  $\gamma = 4$  and  $\gamma = 5$ . At stronger couplings, we see a sharp shift to larger values of  $\gamma$  as the cumulative potential begins to resemble the planar rotor.

*et al.* we see a continuous phase transition at small  $\gamma$  and a first-order transition at large  $\gamma$ . [23] Comparing with our parameter mapping, systems corresponding to smectics with large cone angles show first-order Sm-A–Sm-C phase transitions, while values of  $\gamma$  corresponding to small cone angles show continuous behavior. Our analysis locates the tricritical point in the two-dimensional system between the  $\gamma$  values of 4 and 5 which corresponds to a cone angle of approximately  $40^\circ$ , though this is dependent on the coarse-graining length scale. The phase behavior proves to be robust to weak interlayer planar rotor interactions. To first order, the interlayer coupling stabilizes the Sm-C phase to higher temperatures but does not significantly change the location of the tricritical point.

The first-order phase transition within the spin system, and thus the spherocylinder system, can be understood in the context of defect or vacancy condensation much like phase transition in the standard Potts model [25]. The system free energy is reduced by overlapping disordered regions, producing a depletion-style attraction between disordered domains. This suggests that the first-order phase transition seen in de Vries smectics also originates from a disorder condensation mechanism.

In addition to exploring the phase behavior of the system, we examined the polarization field response of the model. Figure 5 demonstrates the qualitative agreement between the spin model and a series of polarization response curves for de Vries material W530 measured via the polarization reversal current [13,26]. These fits capture the basic sigmoidal behavior over a substantial range of temperatures above the Sm-A–Sm-C phase transition using only three free parameters.

In summary, we have shown that the implications of a hollow cone smectic go further than the layer spacing and electro-optics to which it has been previously applied. The steric interactions inherent in a hollow cone smectic imply  $\phi$ -correlated domains and, at sufficiently large cone angles, a first-order Sm-A–Sm-C phase transition which leads to the observed sigmoidal field response.

Further simulation studies, for example, an atomistic level investigation, are needed to understand the microscopic origins of hollow cone behavior itself. Our work, however, has

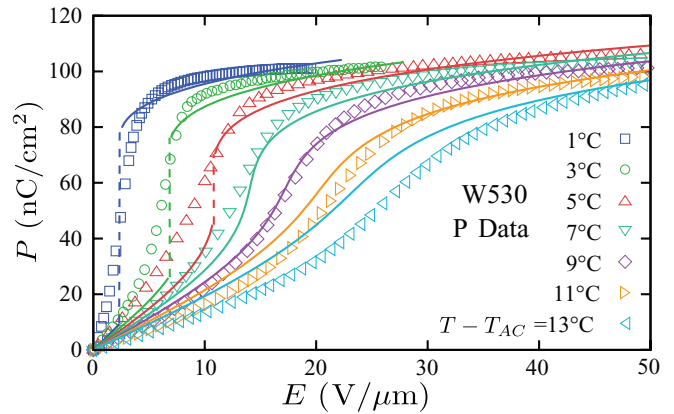


FIG. 5. (Color online) Comparison of the polarization density response of de Vries material W530 (symbols) when an electric field is applied across a liquid-crystal cell with bookshelf alignment [13] and the model's predictions for  $\gamma = 6$  (curves). The model's energy units at a given value of  $\gamma$  are set by equating the model's Sm-A–Sm-C transition temperature  $T_{AC}$  to the transition temperature for W530,  $39^\circ\text{C}$ . The polarization density saturation and susceptibility is scaled to demonstrate simultaneous qualitative agreement with several polarization curves near the Sm-A–Sm-C transition. At lower temperatures we predict a discontinuous change in  $P$  which is not seen experimentally. The continuous experimental behavior may be due to quenched surface disorder in the cell.

shown that once hollow cone behavior is present, first-order behavior emerges naturally as a consequence of excluded volume effects. Even without features such as out-of-layer fluctuations and an atomistic molecular model, we find that our minimal hollow cone model is a microscopic picture of de Vries smectics that encompasses most of the experimentally observed characteristics of the phase including the common first-order phase transition and qualitative agreement with the electro-optics.

We thank Per Rudquist and Leo Radzihovsky for helpful discussions. Funding provided by MRSEC Grant No. NSF DMR 0820579 and Materials World Network Grant No. NSF DMR 1008300.

[1] A. De Vries, *Mol. Cryst. Liq. Cryst.* **41**, 27 (1977).  
 [2] A. De Vries, A. Ekachai, and N. Spielberg, *Mol. Cryst. Liq. Cryst.* **49**, 143 (1979).  
 [3] A. De Vries, *Mol. Cryst. Liq. Cryst.* **49**, 179 (1979).  
 [4] J. P. F. Lagerwall and F. Giesselmann, *Chem. Phys. Chem.* **7**, 20 (2006).  
 [5] N. Kapernaum, D. M. Walba, E. Korblova, C. Zhu, C. Jones, Y. Shen, N. A. Clark, and F. Giesselmann, *Chem. Phys. Chem.* **10**, 890 (2009).  
 [6] J. V. Selinger, P. J. Collings, and R. Shashidhar, *Phys. Rev. E* **64**, 061705 (2001).  
 [7] N. A. Clark, T. Bellini, R. Shao, D. Coleman, S. Bardon, D. R. Link, J. E. Maclennan, X. Chen, M. D. Wand, D. M. Walba *et al.*, *Appl. Phys. Lett.* **80**, 4097 (2002).

[8] D. M. Walba, E. Korblova, L. Eshdat, M. C. Biewer, H. Yang, C. Jones, M. Nakata, M. Talarico, R. Shao, and N. A. Clark, *J. Soc. Inf. Disp.* **15**, 585 (2007).  
 [9] Y. Takanishi, Y. Ouchi, H. Takezoe, and A. Fukuda, *Jpn. J. Appl. Phys.* **28**, L487 (1989).  
 [10] J. C. Roberts, N. Kapernaum, Q. Song, D. Nonnenmacher, K. Ayub, F. Giesselmann, and R. P. Lemieux, *J. Am. Chem. Soc.* **132**, 364 (2010).  
 [11] N. A. Clark (private communication).  
 [12] C. Bahr and G. Heppke, *Phys. Rev. A* **41**, 4335 (1990).  
 [13] L. Wang, D. M. Walba, R.-F. Shao, D. Coleman, M. Nakata, T. Shimmachi, J. E. Maclennan, and N. A. Clark, in *Proceedings of the 21st International Liquid Crystal Conference* (Taylor & Francis, London, 2006).

- [14] S. K. Prasad, D. S. Shankar Rao, S. Sridevi, C. V. Lobo, B. R. Ratna, J. Naciri, and R. Shashidhar, *Phys. Rev. Lett.* **102**, 147802 (2009).
- [15] S. Ghosh, P. Nayek, S. K. Roy, T. Pal Majumder, M. Zurowska, and R. Dabrowski, *Europhys. Lett.* **89**, 16001 (2010).
- [16] W. L. McMillan, *Phys. Rev. A* **4**, 1238 (1971).
- [17] K. Saunders, D. Hernandez, S. Pearson, and J. Toner, *Phys. Rev. Lett.* **98**, 197801 (2007).
- [18] K. Saunders, *Phys. Rev. E* **77**, 061708 (2008).
- [19] M. V. Gorkunov, F. Giesselmann, J. P. F. Lagerwall, T. J. Sluckin, and M. A. Osipov, *Phys. Rev. E* **75**, 060701 (2007).
- [20] M. V. Gorkunov, M. A. Osipov, J. P. F. Lagerwall, and F. Giesselmann, *Phys. Rev. E* **76**, 051706 (2007).
- [21] S. T. Lagerwall, P. Rudquist, and F. Giesselmann, *Mol. Cryst. Liq. Cryst.* **510**, 148 (2009).
- [22] H. Nagata, M. Zukovic, and T. Idogaki, *J. Magn. Magn. Mater.* **234**, 320 (2001).
- [23] E. Domany, M. Schick, and R. H. Swendsen, *Phys. Rev. Lett.* **52**, 1535 (1984).
- [24] P. Chaikin and T. Lubensky, *Principles of Condensed Matter Physics* (Cambridge University, New York, 2000).
- [25] B. Nienhuis, A. N. Berker, E. K. Riedel, and M. Schick, *Phys. Rev. Lett.* **43**, 737 (1979).
- [26] Y. Shen, L. Wang, R. Shao, T. Gong, C. Zhu, H. Yang, J. E. Maclennan, D. M. Walba, and N. A. Clark (private communication).